Low-loss hollow-core silica fibers with adjacent nested anti-resonant tubes

Habib, Selim; Bang, Ole; Bache, Morten

Published in:
Optics Express

Publication date:
2015

Document Version
Publisher's PDF, also known as Version of record

Low-loss hollow-core silica fibers with adjacent nested anti-resonant tubes

Md. Selim Habib, Ole Bang, and Morten Bache*

DTU Fotonik, Department of Photonics Engineering, Technical University of Denmark, DK-2800, Kgs. Lyngby, Denmark

**moba@fotonik.dtu.dk*

Abstract: We report on numerical design optimization of hollow-core anti-resonant fibers with the aim of reducing transmission losses. We show that re-arranging the nested anti-resonant tubes in the cladding to be adjacent has the effect of significantly reducing leakage as well as bending losses, and for reaching high loss extinction ratios between the fundamental mode and higher order modes. We investigate two versions of the proposed design, one optimized for the mid-IR and another scaled down version for the near-IR and compare them in detail with previously proposed anti-resonant fiber designs including nested elements. Our proposed design is superior with respect to obtaining the lowest leakage losses and the bend losses are also much lower than for the previous designs. Leakage losses as low as 0.0015 dB/km and bending losses of 0.006 dB/km at 5 cm bending radius are predicted at the ytterbium lasing wavelength 1.06 μm. When optimizing the higher-order-mode extinction ratio, the low leakage loss is sacrificed to get an effective single-mode behavior of the fiber. We show that the higher-order-mode extinction ratio is more than 1500 in the range 1.0-1.1 μm around the ytterbium lasing wavelength, while in the mid-IR it can be over 100 around λ = 2.94 μm. This is higher than the previously considered structures in the literature using nested tubes.

OCIS codes: (060.4005) Microstructured fibers; (060.2310) Fiber optics; (060.2400) Fiber properties; (060.2280) Fiber design and fabrication.

References and links

1. R. F. Cregan, B. J. Mangan, J. C. Knight, T. A. Birks, P. St. J. Russell, P. J. Roberts, and D. C. Allan, "Single-mode photonic band gap guidance of light in air," Science **285**(5433), 1537–1539 (1999).
2. G. Humbert, J. Knight, G. Bouwmans, P. Russell, D. Williams, P. Roberts, and B. Mangan, "Hollow core photonic crystal fibers for beam delivery," Opt. Express **12**(8), 1477–1484 (2004).
3. F. Gèrôme, P. Dupriez, J. Clowes, J. C. Knight, and W. J. Wadsworth, "High power tunable femtosecond soliton source using hollow-core photonic bandgap fiber, and its use for frequency doubling," Opt. Express **16**(4), 2381–2386 (2008).
4. F. Gérôme, K. Cook, A. K. George, W. J. Wadsworth, and J. C. Knight, "Delivery of sub-100fs pulses through 8m of hollow-core fiber using soliton compression," Opt. Express **15**(12), 7126–7131 (2007).
5. A. Urich, R. R. J. Maier, F. Yu, J. C. Knight, D. P. Hand, and J. D. Shephard, "Flexible delivery of Er:YAG radiation at 2.94 μm with negative curvature silica glass fibers: a new solution for minimally invasive surgical procedures," Biomed. Opt. Express **4**(2), 193–205 (2013).
6. J. Anthony, R. Leonhardt, S. G. Leon-Saval, and A. Argyros, "THz propagation in kagome hollow-core microstructured fibers," Opt. Express **19**(19), 18470–18478 (2011).
7. P. J. Roberts, F. Couny, H. Sabert, B. J. Mangan, D. P. Williams, L. Farr, M. W. Mason, A. Tomlinson, T. A. Birks, J. C. Knight, and P. St. J. Russell, "Ultimate low loss of hollow-core photonic crystal fibres," Opt. Express **13**(1), 236 (2005).
8. F. Benabid and P. J. Roberts, "Linear and nonlinear optical properties of hollow core photonic crystal fiber," J. Mod. Opt. **58**(2), 87–124 (2011).
9. F. Couny, F. Benabid, P. J. Roberts, P. S. Light, and M. G. Raymer, "Generation and photonic guidance of multi-octave optical-frequency combs," Science **318**(5853), 1118–1121 (2007).
10. F. Couny, F. Benabid, and P. S. Light, "Subwatt threshold cw Raman fiber-gas laser based on H_2-filled hollow-core photonic crystal fiber," Phys. Rev. Lett. **99**(14), 143903 (2007).

#240559 Received 8 May 2015; revised 16 Jun 2015; accepted 17 Jun 2015; published 24 Jun 2015

11. F. Couny, F. Benabid, and P. S. Light, "Large-pitch kagome-structured hollow-core photonic crystal fiber," Opt. Lett. **31**(24), 3574–3576 (2006).
12. Y. Y. Wang, F. Couny, P. J. Roberts, and F. Benabid, "Low loss broadband transmission in optimized core-shape Kagome hollow-core PCF," in *Lasers Electro-Optics* (*CLEO*) and *Quantum Electron. Laser Sci.* (*QELS*) 2010, paper CPDB4.
13. Y. Y. Wang, N. V. Wheeler, F. Couny, P. J. Roberts, and F. Benabid, "Low loss broadband transmission in hypocycloid-core Kagome hollow-core photonic crystal fiber," Opt. Lett. **36**(5), 669–671 (2011).
14. M. Alharbi, T. Bradley, B. Debord, C. Fourcade-Dutin, D. Ghosh, L. Vincetti, F. Gérôme, and F. Benabid, "Hypocycloid-shaped hollow-core photonic crystal fiber Part II: cladding effect on confinement and bend loss," Opt. Express **21**(23), 28609–28616 (2013).
15. Y. Wang, M. Alharbi, T. D. Bradley, C. Fourcade-Dutin, B. Debord, B. Beaudou, F. Gerôme, and F. Benabid, "Hollow-core photonic crystal fibre for high power laser beam delivery," High Power Laser Sci. Eng. **1**(01), 17–28 (2013).
16. A. D. Pryamikov, A. S. Biriukov, A. F. Kosolapov, V. G. Plotnichenko, S. L. Semjonov, and E. M. Dianov, "Demonstration of a waveguide regime for a silica hollow--core microstructured optical fiber with a negative curvature of the core boundary in the spectral region > 3.5 μm," Opt. Express **19**(2), 1441–1448 (2011).
17. F. Yu, W. J. Wadsworth, and J. C. Knight, "Low loss silica hollow core fibers for 3-4 μm spectral region," Opt. Express **20**(10), 11153–11158 (2012).
18. A. N. Kolyadin, A. F. Kosolapov, A. D. Pryamikov, A. S. Biriukov, V. G. Plotnichenko, and E. M. Dianov, "Light transmission in negative curvature hollow core fiber in extremely high material loss region," Opt. Express **21**(8), 9514–9519 (2013).
19. W. Belardi and J. C. Knight, "Hollow antiresonant fibers with reduced attenuation," Opt. Lett. **39**(7), 1853–1856 (2014).
20. W. Belardi and J. C. Knight, "Hollow antiresonant fibers with low bending loss," Opt. Express **22**(8), 10091–10096 (2014).
21. F. Poletti, "Nested antiresonant nodeless hollow core fiber," Opt. Express **22**(20), 23807–23828 (2014).
22. A. F. Kosolapov, A. D. Pryamikov, A. S. Biriukov, V. S. Shiryaev, M. S. Astapovich, G. E. Snopatin, V. G. Plotnichenko, M. F. Churbanov, and E. M. Dianov, "Demonstration of CO_2-laser power delivery through chalcogenide-glass fiber with negative-curvature hollow core," Opt. Express **19**(25), 25723–25728 (2011).
23. O. Humbach, H. Fabian, U. Grzesik, U. Haken, and W. Heitmann, "Analysis of OH absorption bands in synthetic silica," J. Non-Cryst. Solids **203**, 19–26 (1996).
24. M. Heiblum and J. Harris, "Analysis of curved optical waveguides by conformal transformation," IEEE J. Quantum Electron. **11**(2), 75–83 (1975).
25. W. Belardi, "New possibilities with hollow core antiresonant fibers," *arXiv:1501.00586*, 2015.

1. Introduction

Hollow-core fibers [1] have attracted a great deal of interest over the past decades owing to their unique ability to confine light in air. These fibers are promising candidates for applications such as high power delivery [2], ultra-short pulse delivery [3], pulse compression [4], mid-infrared (mid-IR) transmission [5], and terahertz applications [6]. Two categories of single-material hollow-core fibers have been studied and designed in the previous decade. The first one is a hollow-core photonic bandgap (HC-PBG) fiber, which guides light via the photonic bandgap effect. The lowest transmission loss reported of this kind of fiber is 1.2 dB/km at 1.62 μm [7]. However, the major limitation of this type of fiber is its limited transmission bandwidth (typically less than 70 THz) [8].

The second fiber category, which guides light via inhibited coupling (IC) between the core and cladding modes [9], include also the so-called hollow-core anti-resonant (HC-AR) fibers. These have "anti-resonant" transmission windows with very low losses. This is because the coupling between the cladding modes and the core mode can be made anti-resonant (strongly inhibited) by carefully engineering the interaction between the cladding modes and the core mode. This type of fiber allows much broader spectral bandwidths than that achieved in HC-PBG fibers. An example of hollow-core fibers guiding via inhibited coupling is the Kagome fiber [10–12]. Several Kagome fibers with different core shapes and sizes have been studied and developed to date for controlling the leakage loss (also known as confinement loss) and modal properties [11,13–15]. The reported results so far in [11,13–15] show that the core shape plays a vital role for the modal content, the power fraction in silica, and the leakage loss. The lowest reported transmission loss of a Kagome fiber was 30 dB/km at 1.55 μm, which was measured in a so-called hypocycloid-core Kagome fiber [15].

#240559 Received 8 May 2015; revised 16 Jun 2015; accepted 17 Jun 2015; published 24 Jun 2015

Other types of HC-AR fibers with low losses have been proposed and developed by several research groups as an alternative optical transmission medium in spectral ranges with high material loss [16–22]. All of the proposed designs have used "negative-curvature" core boundaries (just like the hypocycloid-core Kagome fiber), as these fibers offer broad transmission bands and low losses due to both a low leakage loss and a weak overlap of the core modes with the silica part of the fiber [16–21]. A particularly simple HC-AR fiber design is where a silica capillary has a periodic arrangement of smaller silica "cladding tubes" acting as anti-resonant elements that define the negative-curvature core. It was demonstrated in [16] that such a fiber guides light even at mid-IR wavelengths above 3.5 μm, despite the very high material loss of silica in this spectral regime. In [17] such an HC-AR fiber was fabricated and demonstrated to have a transmission loss of only 34 dB/km at 3.05 μm, and transmission of wavelengths beyond 4 μm was also demonstrated. Light transmission in the spectral range of 2.5 to 7.9 μm through a silica HC-AR fiber with a transmission loss of about 50 dB/km at 3.39 μm has also been realized [18].

Recently, a modified form of HC-AR fibers has been introduced [19], where smaller tubes are nested inside the tubes defining the core. This increases the inhibited coupling between the fundamental core mode and the cladding modes, and thereby the leakage loss is reduced. Leakage losses at 3.05 μm were predicted to be below 0.1 dB/km using a single nested anti-resonant element in each larger tube, and below 0.01 dB/km using a "nested-in-nested" structure with two nested anti-resonant elements in each larger tube. However, due to the large losses of silica at this wavelength the total transmission loss is 3 orders of magnitude larger and the low leakage losses are therefore not exploited fully. Therefore a scaled-down version of the fiber was also investigated in [19] in the near-IR, where leakage loss is the dominant contribution to the transmission loss. Leakage losses below 0.1 dB/km at 1.06 μm were predicted. Moreover, HC-AR fibers with a so-called "node-free" core boundary have been studied [20] in order to reduce the bending loss, where "node-free" refers to the cladding tubes being arranged so they do not touch each other. It was demonstrated in [20] that bending losses are strongly increased by the coupling between the fundamental mode and the cladding modes when the anti-resonant elements are touching each other. It was also shown that bending losses can be improved significantly, in particular when the cladding tube separation is relatively large. More recently [21], also proposed a node-free HC-AR fiber with additional tubes nested inside the original tubes, but with 6 tubes defining the core, and reported a significantly reduced leakage loss in the near-IR (<0.01 dB/km for 2 nested tubes), as well as reduced oscillations in the loss spectrum when compared to the design reported in [19].

In this work, we intend to further investigate and extend the fiber designs reported in [19,21] in order to evaluate its benefits in terms of loss reduction. Our main motivation is to find a fiber design capable of broadband low-loss mid-IR transmission, but we will also investigate the performance in the near-IR in a scaled-down version of the mid-IR fiber. Our design is also based on nested anti-resonant elements, but instead of multiple "nested-in-nested" tubes we suggest a design with adjacent nested anti-resonant (ANAR) tubes. We find that re-arranging the cladding anti-resonant tubes in this way helps to reduce both leakage and bending losses significantly, and offers an extra degree of freedom needed for increasing the extinction loss ratio of the fundamental mode to the higher-order modes, which when high enough gives an effective single-mode operation. The proposed hollow-core ANAR fiber can therefore offer record-low leakage loss in the near and mid-IR spectral regions, wide transmission bandwidth, and effectively single mode operation. Finally, as all HC-AR fibers it has a very weak overlap of the mode-field with the silica, which makes it a very suitable candidate for high-power delivery.

#240559 Received 8 May 2015; revised 16 Jun 2015; accepted 17 Jun 2015; published 24 Jun 2015

2. Numerical analysis

We begin by describing the parameters chosen for the mid-IR fibers. We used for all our numerical simulations a core radius of R_c = 47 μm (defined as the maximum radius of a circle that can be inscribed inside the core), which is identical to the fiber structure reported experimentally in [17] and simulated in [19]. However, in contrast to those we have chosen to use a silica strut thickness of t = 1.26 μm, which gives an anti-resonant first-order transmission window in the high-frequency mid-IR range (specifically around λ = 2.94 μm, the emission wavelength of Er:YAG lasers). This is because we found a superior loss-performance by choosing operation in the first transmission window instead of the second. For the same reason we choose also throughout this paper to use six anti-resonant tubes instead of eight in all designs. Figure 1 shows the four considered designs, all optimized to give minimal leakage loss at λ = 2.94 μm. Figure 1(a) shows the geometry of a "typical" HC-AR fiber [16] with six anti-resonant tubes in a node-free configuration. The modified HC-AR fibers, originally investigated in an 8-ring configuration by Belardi *et al*. [17] and later in a 6-ring configuration by Poletti [21], are shown in Figs. 1(b)-1(c), using the nested (b) and nested-in-nested (c) configurations. Our proposed alternative ANAR design is shown in Fig. 1(d), using node-free outer cladding tubes and multiple adjacent nested elements. In our ANAR design the six outer capillary tubes have diameter d_o and a perimeter distance between them of 4 μm, i.e. as in design (a). The nested elements are chosen as three adjacent tubes with inner air-hole diameter of d_i. The first nested tube is placed in the radial direction at the internal edge of the outer tube, while the two other nested tubes are placed along the direction of a line passing through the outer tube center and orthogonally to the radial direction. In this configuration optimized to give lowest leakage losses the angle between the center and the adjacent nested tubes is therefore 90°, but we will also investigate configurations where this angle is changed. The inner air-hole diameter d_i and cladding air-hole diameter d_o in the optimized design is 32 μm and 86 μm, respectively. The perimeter separation between the inner air-holes is 2.35 μm. The inner and outer air-hole tubes are arranged in a node-free design, as the presence of nodes generates large oscillations with spectral periods of a few nanometers [21]. Moreover, the node-free design is known to reduce the leakage loss [21].

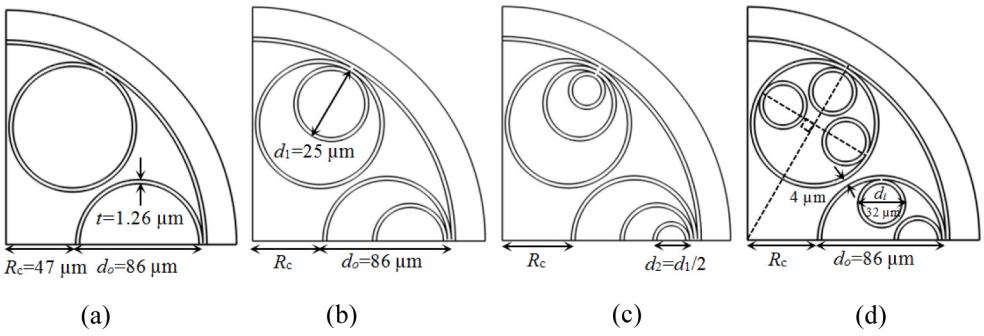

Fig. 1. Geometries considered in the mid-IR simulations. (a) Typical optimized HC-AR fiber design with six circular tubes; (b)-(c) the nested ("1AE", i.e. one anti-resonant element) and nested-in-nested ("2AE", i.e. two anti-resonant elements) designs proposed in [21] in which d_1 = 25 μm and $d_2 = d_1/2$; (d) our proposed adjacent nested anti-resonant (ANAR) structure with three adjacent nested anti-resonant tubes. All fibers have the same core radius R_c = 47 μm and uniform silica strut thickness t = 1.26 μm.

We used the finite-element method based commercial software COMSOL for our numerical simulations. Perfectly-matched layer boundary conditions were used to accurately calculate the leakage loss. In order to model HC-AR fibers accurately, great care must be taken to optimize both mesh size and perfectly-matched layer parameters [21]. To ensure convergence of the numerical results, the code was tested by reproducing the results of [19–

#240559 Received 8 May 2015; revised 16 Jun 2015; accepted 17 Jun 2015; published 24 Jun 2015

21], and therefore we are able to here present our own calculations of the designs proposed in the literature and shown in Figs. 1(a)-1(c).

2.1 Transmission loss in the mid-IR

Figure 2 shows the loss spectrum of the four considered structures. In our calculations, the fraction of power in silica was calculated to estimate the effective material loss and then added to the leakage loss to obtain the total transmission loss. The material loss of silica was taken from [23]. The broken black line shows the calculated leakage loss of a "typical" optimized HC-AR fiber in which the minimum leakage loss is ~21 dB/km, which is limited by coupling to the voids in the cladding [19]. The broken green and blue lines show the leakage loss of the modified forms proposed in [19] and shown in Figs. 1(b)-1(c), in which nested anti-resonant elements were used to reduce the leakage loss. The minimum leakage losses are ~0.03dB/km and ~0.0039dB/km at 2.94 μm for 1AE and 2AE, respectively. Finally, the broken red line shows the loss spectrum of our proposed ANAR fiber, in which the minimum leakage loss is about 0.0009 dB/km. Thus, the nested designs have losses several orders of magnitude lower than the "typical" HC-AR fiber and with the ANAR design giving the best performance having the lowest loss in the range 2.75-3.2 μm. That being said, the loss is clearly dominated by material loss, despite the low power fraction in silica, making the transmission loss practically identical for the 3 different nested designs.

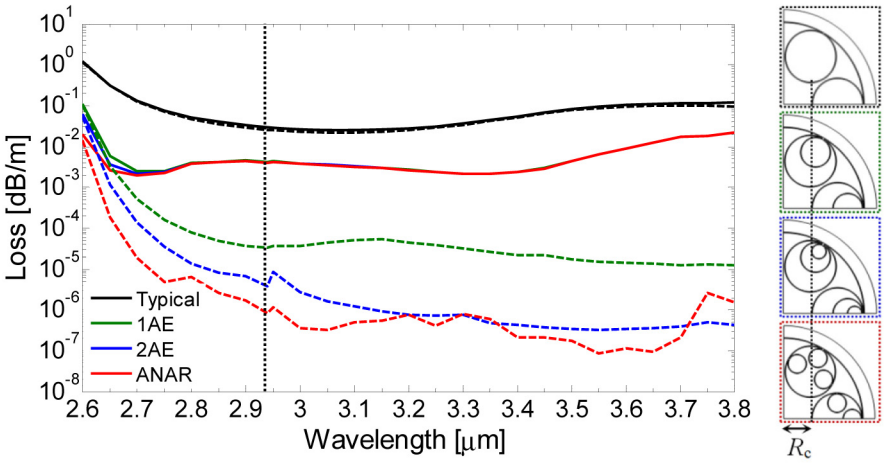

Fig. 2. Calculated loss spectra. The broken lines indicate leakage loss while solid lines show the transmission loss where the material loss of silica is included. All structures have the same core radius R_c = 47 μm and uniform silica strut thickness t = 1.26 μm. The color of the frame corresponds to the color of the line in the plot. The thin dotted line indicates the wavelength for which the losses are optimized.

2.2 Bending losses in the mid-IR

In order to calculate the bending loss, the bent structure is transformed into its equivalent straight structure with equivalent refractive index profile, n_{eq} defined by [24]

$$n_{eq} = n(x,y)\,exp(x/R_b) \tag{1}$$

where R_b is the bending radius, x is the transverse distance from the center of the fiber, $n(x,y)$ is the refractive index profile of the straight fiber. The bending losses were calculated at 2.94 μm and the bending direction was chosen along the x-axis giving the bend-loss curve shown in Fig. 3. A significant improvement of the bending loss was found for the proposed ANAR fiber (dashed red curve), for which the bending leakage loss is several orders of magnitude

#240559 Received 8 May 2015; revised 16 Jun 2015; accepted 17 Jun 2015; published 24 Jun 2015

lower than the typical HC-AR fiber and even one order of magnitude lower than the 1AE and 2AE fibers for bend radii between 5 and 15 cm and the leakage loss is only weakly changing for bend radii above ~15 cm. Again, as with the transmission loss above, the performance is dominated by material loss, making the bending loss curves of all three nested designs identical for larger bend radii when the material loss is included (solid lines). However, for low bending radius the "typical", 1AE, and 2AE structures have high loss peaks, whereas no loss peaks are observed for the ANAR structure, which results in very limited increase in transmission loss when the fiber is bent.

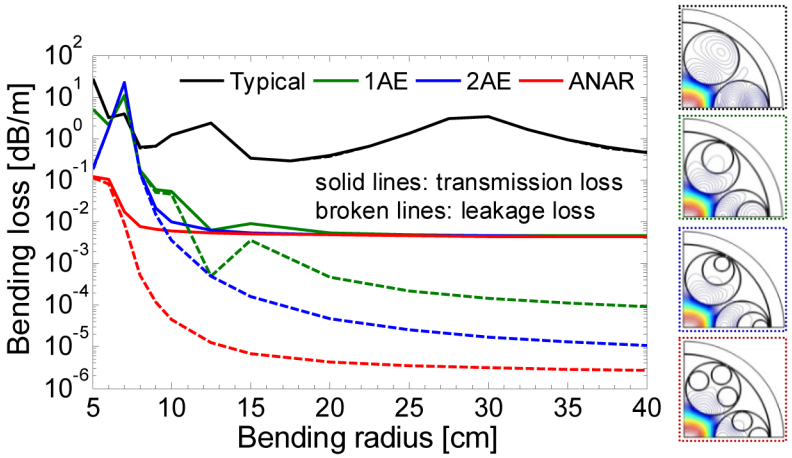

Fig. 3. Calculated bending loss at 2.94 μm versus bending radius. Note that black solid and broken lines are coincident. The contour plots of the fundamental air-core mode distribution are shown in the right hand side for a 10 cm bending radius. The color of the frame corresponds to the color of the line in the plot.

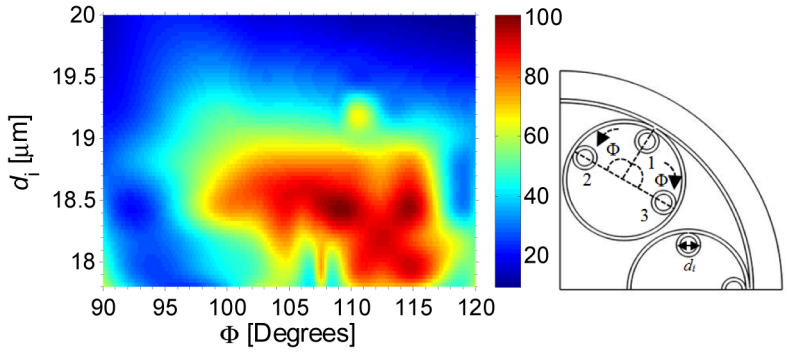

Fig. 4. Calculated HOMER of the proposed ANAR with different values of d_i as a function of Φ, which is the angle between adjacent inner tubes 2 and 3 and tube 1, while keeping the position of tube 1 fixed as before. The simulations are performed at λ = 2.94 μm.

2.3 Effectively single-modeness in the mid-IR

HC-AR fibers are typically not single-moded due to the large core, but may be designed to have higher losses of the higher-order modes (HOMs) so that the fiber is effectively single-moded. Figure 4 shows how free design parameters of the ANAR fiber can be controlled to optimize the so-called higher-order-mode extinction ratio (HOMER), which is defined as the ratio between the transmission loss of the HOM having the lowest transmission loss and the transmission loss of the fundamental mode (FM). The optimization of HOMER is performed by symmetrically changing the angle Φ between the adjacent nested tubes and the central

#240559 Received 8 May 2015; revised 16 Jun 2015; accepted 17 Jun 2015; published 24 Jun 2015

nested tube, which is kept fixed, and the inner air-hole diameter d_i. As Fig. 4 shows the optimum HOMER is found to be around 100 at Φ = 109 degrees and d_i = 18.4 µm.

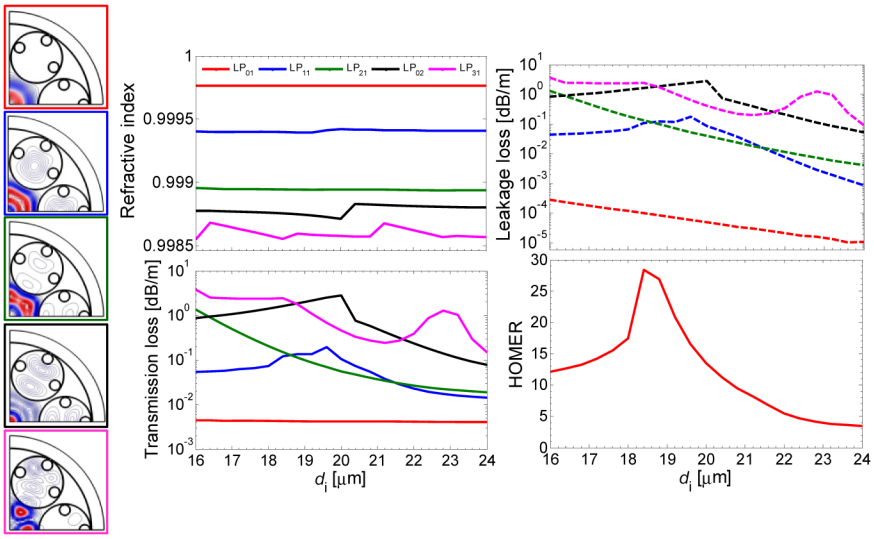

Fig. 5. Effect of changing the inner air-hole diameter d_i with a fixed R_c = 47 µm, t = 1.26 µm, d_o = 86 µm, Φ = π/2 and wavelength 2.94 µm. Contour plots of the first five core modes are shown on the left hand side for 18.4 µm inner air-hole diameter (where the maximum HOMER value is found). The color of the frame corresponds to the color of the line in the plot.

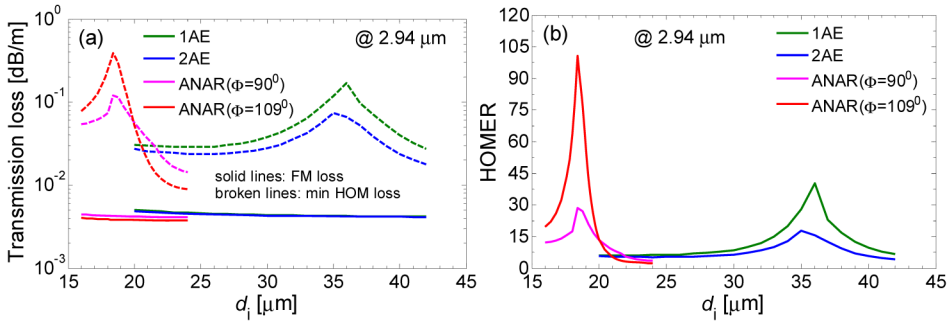

Fig. 6. Calculated (a) transmission loss and (b) HOMER as a function of d_i for 1AE, 2AE and ANAR structures. The simulations are performed at λ = 2.94 µm.

In order to better understand how the fiber design affects the HOMER, Fig. 5 shows the refractive index, leakage loss, and transmission loss of the first five core-guided modes (LP_{01}, LP_{11}, LP_{21}, LP_{02}, and LP_{31}) as a function of the inner air-hole diameter d_i from 16 to 24 µm with a fixed R_c = 47 µm, t = 1.26 µm, d_o = 86 µm, and Φ = π/2. It can be seen that the effective refractive indices of the core modes do not change much as a function of the inner air-hole diameter. This is obvious, as they depend mainly on the fiber core radius, which is kept constant. Instead, the leakage loss of the LP_{01} mode can clearly be reduced significantly by increasing the inner air-hole diameter. Comparing the figures with the leakage and transmission loss we see that the HOMs have so high leakage loss that it dominates the transmission loss, while for the FM is it the other way around. What is interesting is that while a large inner air-hole diameter d_i gives the lowest leakage loss, it does not give the largest HOMER value. For the ANAR structure a HOMER just above 5 is found for large air-hole diameters above 22 µm. However, when decreasing the inner air-hole diameter away from the optimal point of lowest leakage loss the HOMER value increases many-fold. This is

#240559 Received 8 May 2015; revised 16 Jun 2015; accepted 17 Jun 2015; published 24 Jun 2015

because the leakage losses of the HOMs increase faster than that of the FM. In other words, by sacrificing a low leakage loss one can get a higher HOMER.

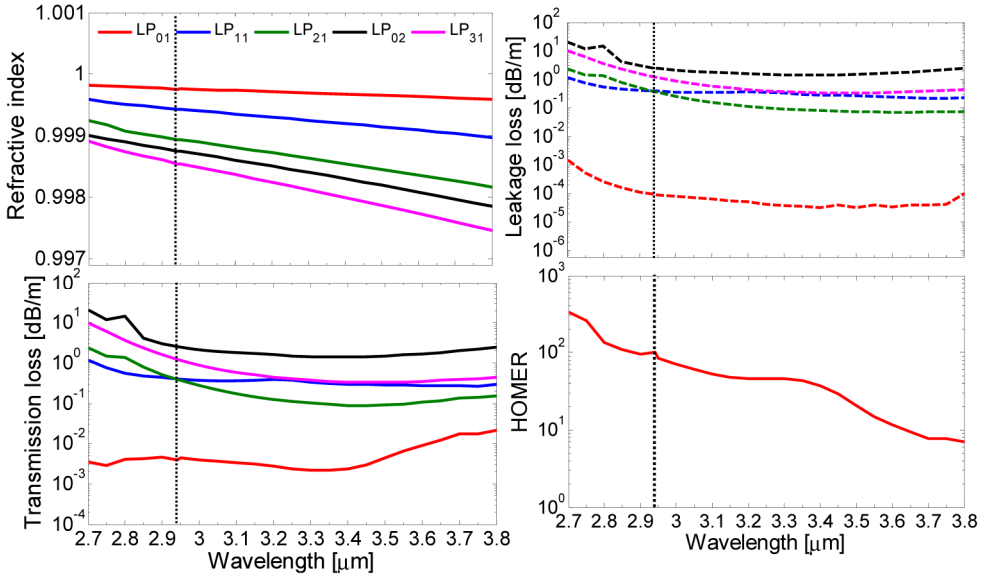

Fig. 7. Wavelength dependence of refractive index, leakage loss, transmission loss and HOMER with a fixed R_c = 47 μm, t = 1.26 μm, d_o = 86 μm, and Φ = 109 degrees for a 18.4 μm inner air-hole diameter. HOMER was calculated with losses in silica taken into account, i.e. using the transmission loss curves.

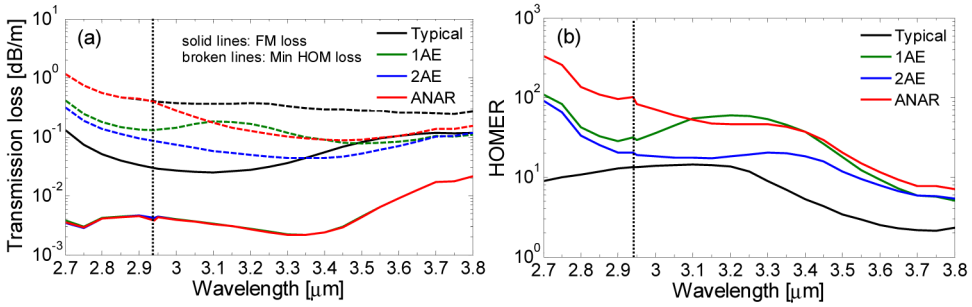

Fig. 8. Comparing the wavelength dependence of (a) transmission loss of the FM and (b) HOMER for all the considered structures. The ANAR parameters are the same as Fig. 7.

Figure 6 shows the transmission loss and HOMER as a function of inner air-hole diameter d_i at 2.94 μm for 1AE, 2AE and ANAR structures. In this case the $d_i = d_1$ in the 1AE and 2AE structures, and for the 2AE structure the ratio $d_2 = d_1/2$ was kept fixed. It can be seen from Fig. 6(a) that for all considered structures the FM loss is roughly constant whereas the HOM loss changes significantly with d_i. Therefore, HOMER strongly depends on d_i which is shown in Fig. 6(b), and the added degree of freedom in the ANAR design in varying the angle turns out to be decisive for obtaining a HOMER level higher than the 1AE and 2AE designs. We note that a similar possibility is offered for the 2AE design, however, we checked that by allowing the diameters of the nested tubes to vary independently, one could not increase HOMER much beyond the level shown in Fig. 6, for which $d_2 = d_1/2$ was kept fixed.

Figure 7 shows the wavelength dependence of the refractive index, leakage loss, transmission loss and HOMER for the ANAR design optimized for maximum HOMER at 2.94 μm. It shows that HOMER can be made in excess of 50 in the entire spectral regime 2.7-

#240559 Received 8 May 2015; revised 16 Jun 2015; accepted 17 Jun 2015; published 24 Jun 2015

3.1 μm. The highest HOMER of about 330 is obtained at 2.7 μm, close to the resonant regime where the transmission losses are very high. Therefore having such a high HOMER implies an increased transmission loss, so again there is a compromise between loss and HOMER.

Figure 8 shows the wavelength dependence of the transmission loss of the FM and the HOMER for all considered structures; each of them has been optimized to give the highest HOMER value at 2.94 μm. It can be seen from Fig. 8(b) that the ANAR design has higher HOMER compared to the typical, 1AE and 2AE structures in the spectral range 2.7-3.1 μm.

2.4 Performance analysis in the near-IR

In the mid-IR the transmission loss performance was dominated by material loss. We now turn our attention to the near-IR, where material loss can be neglected. As a representative example, we choose to explore the ANAR performance at λ = 1.06 μm, and to do so we start out by simply scaling down the fiber structural parameters by a factor of 3 in all four designs presented in Fig. 1 (this approach was also taken in [19]; the strut thickness of our scaled-down design is also identical to that of [17]). These scaled-down fibers turn out to give the lowest leakage loss at 1.06 μm, and can therefore not be optimized further. The measured loss of dry F300 silica is of the order of 10^{-3} dB/m [23] or less in the wavelength range between 0.95 and 1.40 μm. The calculated power fraction in silica of the optimum ANAR structure with the lowest leakage loss is less than 10^{-4} in this spectral regime, and similar values are found for the 1AE and 2AE structures. Therefore, the transmission loss will practically be equivalent to the leakage loss.

From the leakage loss spectrum shown in Fig. 9(a) we see that the ANAR fiber has a leakage loss of 0.0015 dB/km at 1.06 μm, which is significantly lower than 1AE and roughly a factor of 2 lower than 2AE. It is remarkable to see that the lowest leakage loss is not found at λ = 1.06 μm, where the design is optimized for, but at a longer wavelength for all nested designs. This shows that the predicted minimum only holds for the simple "typical" design and that for the nested designs perhaps a smaller strut thickness could be considered as to move this minimum towards the chosen target wavelength.

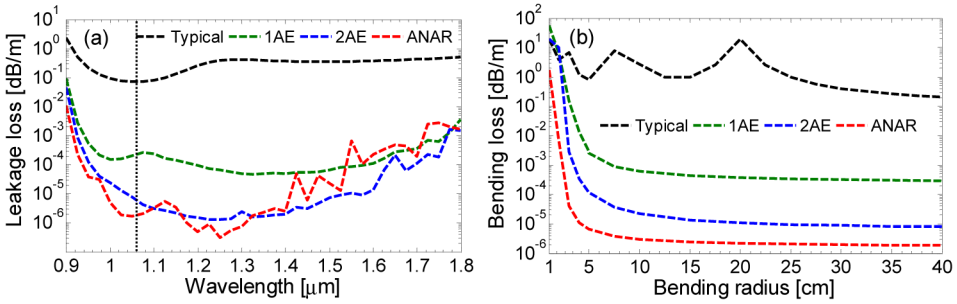

Fig. 9. Calculated leakage loss spectra (a) and bending loss (b) as a function of bending radius at λ = 1.06 μm. The fiber parameters have been scaled down by a factor of 3 ($t' = t/3$, $R_c' = R_c/3$, $d_o' = d_o/3$, and $d_i' = d_i/3$) and in the ANAR design Φ = π/2 was used.

The bending loss for the scaled fiber structures at 1.06 μm is presented in Fig. 9(b), which shows that the bending losses of the three fibers with nested elements are almost constant for reasonable bend radii. Figure 9(b) also confirms that the ANAR design has a bend loss below 0.006 dB/km at 5 cm bending radius, which is about one and two orders of magnitude lower than that of the 1AE and 2AE fibers, respectively. Most importantly, the ANAR design shows low bending loss even at a very small bending radius of 1 cm compared to the 1AE and 2AE fibers, at a level which is even comparable to an HC-PBG fiber.

We have also optimized HOMER in the near-IR in the 2D design parameter space of the ANAR fiber, and Fig. 10(a) shows again that both Φ and d_i have a strong effect on HOMER.

#240559 Received 8 May 2015; revised 16 Jun 2015; accepted 17 Jun 2015; published 24 Jun 2015

The optimum HOMER is found to be in excess of 2500 at Φ = 109 degrees and d_i = 6.0 μm. Interestingly, we note that the optimum angle Φ is the same in both near and mid-IR.

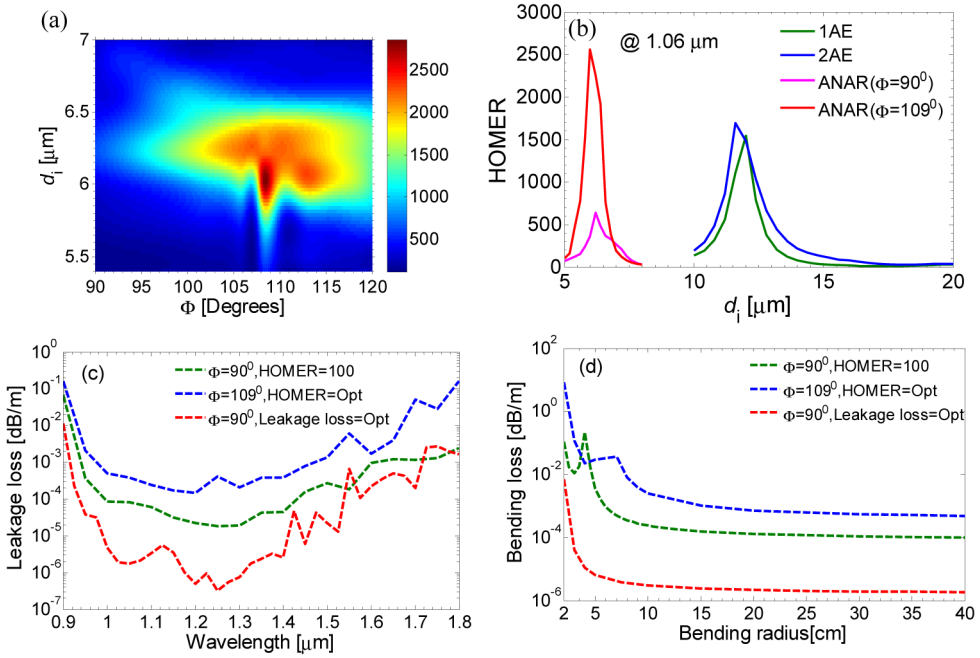

Fig. 10. Calculated HOMER of the proposed ANAR structure versus diameter d_i and angle Φ (a). HOMER versus d_i, for the 1AE and 2AE structures and the ANAR design with Φ = 90° and optimum Φ = 109°. Leakage loss (c) and bending loss (d) for the ANAR design optimized for maximum HOMER, a design chosen to give an intermediate HOMER, and a design optimized to give the lowest leakage loss. The simulations of (a), (b), and (d) are performed at λ = 1.06 μm.

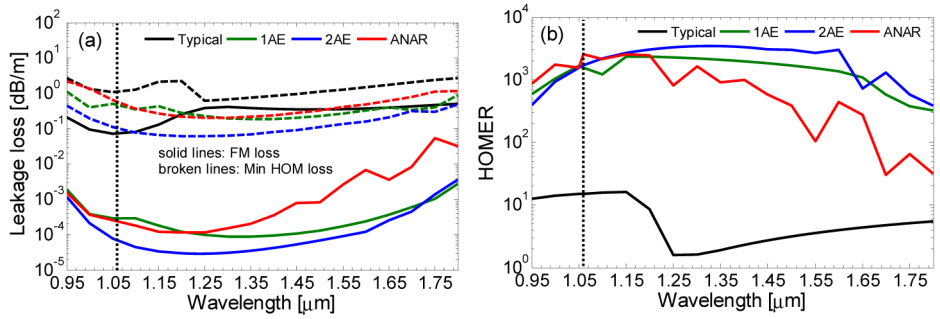

Fig. 11. Wavelength dependence of (a) leakage loss and (b) HOMER for the optimized parameters. The optimum design parameters are: $t' = t/3$, $R_c' = R_c/3$, $d_o' = d_o/3$, and d_i = 6μm,12μm, and 11.6μm for ANAR, 1AE, and 2AE respectively, and in the ANAR design Φ = 109 degrees was used.

The effect of the inner air-hole diameter d_i on HOMER at 1.06 μm for the considered structures is shown in Fig. 10(b). All three structures show that an optimized design can lead to well over 30 dB extinction ratio, and the largest HOMER is found in the ANAR design with Φ = 109 degrees. It is important to remember that this optimization comes at the price of an increased leakage loss, as illustrated in Fig. 10(c), where we compare the ANAR design with maximum HOMER (Φ = 109°, d_i = 6.0 μm) with the Φ = 90° design with lowest leakage

#240559 Received 8 May 2015; revised 16 Jun 2015; accepted 17 Jun 2015; published 24 Jun 2015

loss (d_i = 10.67 µm) and a third design for which HOMER = 100 (Φ = 90°, d_i = 7.4 µm). It can be seen from Fig. 10(c) that the optimum HOMER design has the highest leakage loss. The bending loss as a function of bending radius is shown in Fig. 10(d). Figure 10(d) shows that optimum HOMER corresponds to higher bending loss.

Figure 11 shows the spectral dependence of the leakage loss of the FM, the minimum HOM loss, and the HOMER in the near-IR. Notably, HOMER is higher than 1000 in the range of 0.96-1.2 µm and more than 1550 in the range 1.0-1.1 µm for an inner air-hole diameter of 6 µm, which makes the fiber effectively single-moded in the near-IR spectral regime. Also the 1AE and 2AE designs have excellent HOMER performances, and especially the 2AE has the highest HOMER and keeps a very high level over a broad wavelength range, and at the same time it has a lower leakage loss than 1AE and ANAR.

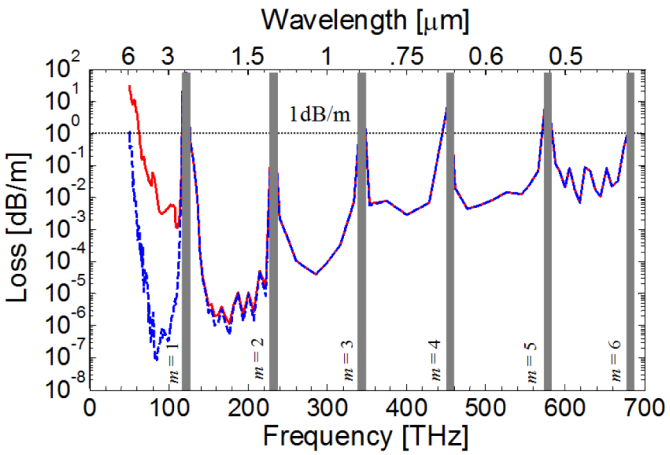

Fig. 12. Numerically found transmission bands in the visible to mid-IR spectral region for the ANAR fiber with R_c = 47 µm, t = 1.26 µm, d_i = 32 µm, d_o = 86 µm, and Φ = 90 degrees. The gray areas indicate high loss regions. The broken blue line indicates leakage loss while solid red line shows the transmission loss where the material loss of silica is included.

2.5 Predicted transmission bands in the near and mid-IR

As mentioned above, the guidance mechanism of our proposed design is based on the anti-resonant effect. Light is guided in silica struts at resonant wavelengths, whereas it is reflected back in the core at anti-resonant wavelengths. The transmission bands can be shifted by scaling the strut thickness of silica, since the cut-off wavelengths depend on the silica strut thickness. The position of the transmission windows are accurately predicted by [9]

$$\lambda_{c,m} = (2/m)t\sqrt{n^2-1} \qquad (2)$$

where m is the resonance order or radial order of the guided mode, t is the thickness of the silica struts, and n is the refractive index of silica. We now consider the performance of our proposed ANAR fiber in the whole near-IR to mid-IR region of 0.44-6 µm for a fixed strut thickness of t = 1.26 µm, as used in the mid-IR sections above. Our modelling results, which are given in Fig. 12, show that there are six low-loss transmission windows in this visible to mid-IR wavelength regime. Remarkably it is possible to have below 1 dB/m total transmission loss over a decade, with a similar performance being expected of the 2AE design, as it offers similar leakage-loss performance. The positions of the transmission bands are accurately predicted by Eq. (2). For example, for a modal order of m = 2 and strut thickness t = 1.26 µm, Eq. (2) predicts a cut-off wavelength around 1.32 µm, which is in excellent agreement with the 1.32 µm observed in Fig. 12.

#240559 Received 8 May 2015; revised 16 Jun 2015; accepted 17 Jun 2015; published 24 Jun 2015

2.6 Fabrication tolerances

In designing HC-AR fibers it is important to demonstrate a good degree of robustness towards imperfections in the fabrication. As was recently done by Belardi [25], we here consider robustness towards a uniform shift of the positions of the three nested tubes as a whole. From the SEM images in [25] such shifts in the position of the nested tube are apparent. Realistically, the shifts would be random from tube to tube, but nevertheless an investigation with a uniform shift will give an indication of the fabrication tolerances that can be allowed during the preform stacking preparation of this fiber type. The uniform shift of the nested tubes is denoted by the angle θ, as sketched in Fig. 13, and as seen there the leakage loss vs. θ at λ = 2.94 μm shows little variation when the angle varies quite significantly from 0° to 45°. When the angle is beyond 45°, the leakage loss increases significantly, indicating that a shift of 45° can be tolerated. In the similar numerical work of Belardi the same qualitative behavior was observed and this maximum tolerance angle was found to be 30° [25].

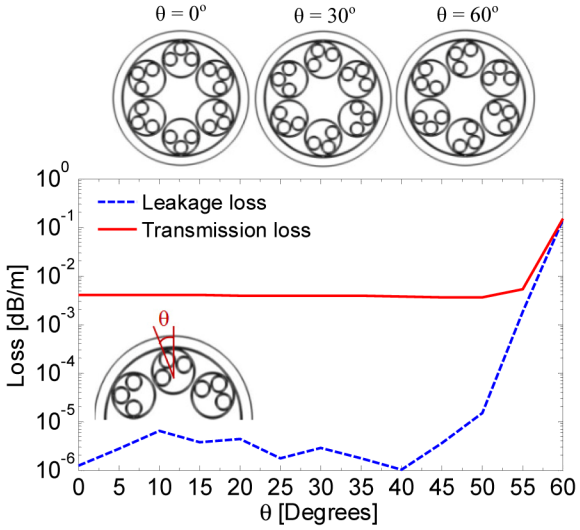

Fig. 13. Predicted fabrication tolerances of the proposed ANAR fiber. The leakage loss is almost stable between 0° to 45°. The simulations were performed at λ = 2.94 μm.

3. Conclusion

In conclusion, we have numerically investigated a novel hollow-core fiber based on the anti-resonant reflecting guiding mechanism. In our proposed design the larger cladding tubes have three smaller adjacent nested anti-resonant (ANAR) tubes inside them, in contrast to earlier studies, where additional nested tubes were nested inside the larger nested tube. We considered two scaled versions of the same fiber design, one where the strut thickness was optimized for transmission in the mid-IR around λ = 2.94 μm, and one where the strut thickness was reduced by a factor of 3 to allow near-IR transmission around λ = 1.06 μm. These cases represent the behavior in the high-loss regime and the low-loss regime of the cladding material, respectively. Each case has its challenges and solutions, but our results and discussions remain quite general and can therefore easily be used for other wavelengths and/or materials for the glass cladding.

We have studied the effects of the ANAR tubes on the fiber losses and modal properties. More specifically on the single-modeness of the ANAR fiber, we found that the higher-order-mode extinction ratio (HOMER) can be over 1500 in the near-IR in the range λ = 1.0-1.1 μm, and around 100 in the mid-IR at λ = 2.94 μm. In comparison, the structures with nested tubes from the literature had lower HOMER values. We found that the high-HOMER design has

#240559 Received 8 May 2015; revised 16 Jun 2015; accepted 17 Jun 2015; published 24 Jun 2015

leakage losses that are increased significantly compared to the lowest level, but still it should be stressed that the leakage losses can be kept at a tolerable level. This can be attributed to the very low leakage loss of the optimal fiber design in the first place. Interestingly, the best overall near-IR performance was found in an optimized nested-in-nested design (2AE), which combined a high HOMER over a broad bandwidth with low leakage losses.

In our simulations we carefully optimized the size and placement of the ANAR elements. In particular for achieving a high HOMER level it was important to find the optimal angular position of the adjacent nested elements with respect to the center nested element and to adjust the diameter of the nested tubes; this optimization came at the expense of a higher leakage loss. The leakage losses were typically optimized by fine-tuning of the diameter of the nested tubes. Instead a rotation of the entire ANAR structure did not seem to influence the results much, which indicates that the design is quite robust towards fabrication variations.

The ANAR fiber when optimized to give the lowest leakage loss offers extremely low bending losses in near-IR even for a bend radius as low as 1 cm. The bend-loss levels are comparable to the HC-PBG fiber and would therefore be suitable for applications.

When comparing the performance of the ANAR design with the earlier proposed designs [19], we generally found that at a given target wavelength the ANAR design could outperform the design with a single nested anti-resonant element (1AE) and the design with a nested-in-nested element (2AE). In optimizing the designs the additional degree of freedom offered by the ANAR and 2AE designs was important to fine-tune the performance. It seems clear that the additional nested element(s) of the ANAR and 2AE designs allow for a stronger inhibited coupling of the core mode to the cladding modes than the 1AE design, which explains the lower losses obtained. From a production point-of-view, the 1AE design has already been realized [25], and in some sense the ANAR design is a generalization of this structure. Thus, we believe the ANAR fiber should be easier to make than the 2AE design.

Given the results presented in this paper, we believe that the proposed ANAR design offers significant advantages and improvements over current designs, promising excellent performance for various applications in near and mid-IR wavelength regimes. We here used the well-known silica platform due to the many advantages it can offer in terms of production, cost etc., but we found that the record-low level of leakage loss was not fully exploited in the mid-IR due to the extremely high material loss of silica. It is therefore an obvious next step to consider the ANAR design based on a mid-IR transparent glass whereby the material losses are reduced to a level comparable to the low leakage losses promised by this design. This in turn would give record low bending losses and much higher HOMER levels. Considering the structural dimensions of the proposed fiber in the mid-IR (100 μm core diameter and outer tube diameter, 30 μm nested tube diameter and >1 μm strut thickness) this should not be a challenge for soft glass fiber technology.

Acknowledgements

The authors acknowledge fruitful discussions with F. Poletti, W. Belardi, and C.C. Wang.

#240559 Received 8 May 2015; revised 16 Jun 2015; accepted 17 Jun 2015; published 24 Jun 2015